Research Article

Josh Lofy, Vladimir Gasparian, Zhyrair Gevorkian, and Esther Jódar[1]*

Faraday and Kerr Effects in Right and Left-Handed Films and Layered Materials

https://doi.org/10.1515/rams-2020-0032
Received Sep 22, 2019; accepted May 13, 2020

Abstract: In the present work, we study the rotations of the polarization of light propagating in right and left-handed films and layered structures. Through the use of complex values representing the rotations we analyze the transmission (Faraday effect) and reflections (Kerr effect) of light. It is shown that the real and imaginary parts of the complex angle of Faraday and Kerr rotations are odd and even functions for the refractive index n, respectively. In the thin film case with left-handed materials there are large resonant enhancements of the reflected Kerr angle that could be obtained experimentally. In the magnetic clock approach, used in the tunneling time problem, two characteristic time components are related to the real and imaginary portions of the complex Faraday rotation angle θ. The complex angle at the different propagation regimes through a finite stack of alternating right and left-handed materials is analyzed in detail. We found that, in spite of the fact that Re(θ) in the forbidden gap is almost zero, the Im(θ) changes drastically in both value and sign.

Keywords: left-handed materials, metamaterials, Faraday rotation angle, Kerr effect, polarization of light

1 Introduction

Negative refractive index magneto-optical metamaterials, also called left-handed materials (LHM), are a new type of artificial material characterized by having a permittivity ϵ and permeability μ both negative [1–3]. The double negative nature of the parameters ϵ and μ at first sight should not affect the refractive index $n = \sqrt{\epsilon\mu}$, as it appears that n should remain positive. However, if complex parameters ϵ and μ have negative non-zero real parts and positive non-zero imaginary parts (where the positive imaginary portion is required for passive materials) the real portion of n will also be negative. Indeed, the permittivity ϵ and the permeability μ, as complex quantities, can be written in the form $\epsilon = r_\epsilon e^{i\theta}$ and $\mu = r_\mu e^{i\phi}$. Accordingly, the refractive index n has the form $n = \sqrt{r_\epsilon r_\mu}e^{i(\theta+\phi)/2}$. The requirement that the imaginary part of the refractive index n must be positive for a non-absorbing medium leads to double inequalities: $0 \le (\theta + \phi)/2 < \pi$. Taking into account the mentioned double inequalities and using the fact that the real parts of ϵ and μ must be both negative (*i.e.* $\cos\theta < 0$ and $\cos\phi < 0$) we get another inequalities: $\pi/2 \le (\theta + \phi)/2 < \pi$. The latter indicates, that the double negative nature of the parameters ϵ and μ affects the refractive index n in the way that the real part of n of a metamaterial, that is $Ren \equiv \sqrt{\epsilon\mu}\cos(\theta+\phi)/2$, is negative (see, *e.g.* Ref. [4] for more details). LHM have multiple uses that include: the ability to resolve images beyond the diffraction limit [5, 6], act as electromagnetic cloaks for particular frequencies of light [7–9], enhance quantum interference [10] or yield to slow light propagation [11]. LHM used also for digital applications possess various exotic functionalities, such as anomalous reflections, broadband diffusion, polarisation conversion [12] and encoding information [13].

The presence of negative indices of refraction in one-dimensional (1D) disordered metamaterials strongly suppresses Anderson localization due to the lack of phase accumulation during wave propagation, which thus weakens interference effects necessary for localization [14]. As a consequence, an unusual behaviour of the localization length ξ at long-wavelengths λ has been observed [14–16]. This is unlike the well-known quadratic asymptotic behaviour $\xi \sim \lambda^2$ for standard isotropic layers (see, *e.g.* [17]). It can be seen that the metamaterial configurations have an effect on the magneto-optical transport properties of the electromagnetic waves. Particularly, the sign of the plane polarization rotation angle in a left-handed medium (LHM) is opposite to the sign of the rotation angle in a

***Corresponding Author: Esther Jódar[1]:** Dpto. Física Aplicada, Antiguo Hospital de Marina, Campus Muralla del Mar. UPCT, Cartagena 30202 Murcia, Spain; Email: esther.jferrandez@upct.es; Tel.: +34 968338925; Fax +34968325337
Josh Lofy, Vladimir Gasparian: Department of Physics, California State University, Bakersfield, CA 93311, United States of America
Zhyrair Gevorkian: Yerevan Physics Institute, Yerevan, Armenia and Institute of Radiophysics and Electronics, Ashtarak-2, 0203, Armenia

right-handed medium (RHM). The Faraday and Kerr rotations (FR and KR) are non-reciprocal polarization rotation effects in which the sign of the rotation is always related to the direction of the magnetic field. This is different in optically active media where the rotation of the polarization is related to the direction of the wave vector. Thus, the non-reciprocity of the Faraday and Kerr effects allow light to accumulate rotations of the same sign and magnitude for both forward and backward propagation and can be enhanced even further by additional round-trip reflections through the medium.

If we assume no absorption and neglect the influence of the boundaries of the system, then in bulk materials for a given ϵ, μ, Verdet constant V and length of medium L, for a constant linear magnetic field B, the Faraday rotation angle is given by $\theta = \frac{LVB\omega}{2c}\sqrt{\frac{\mu}{\epsilon}}$. When the reflections within the boundaries are relevant the outgoing reflected wave is generally elliptically polarized, with or without absorption. The major axis of the ellipse is rotated with respect to the original direction of polarization and the maximum FR (KR) angle does not necessarily coincide with angular frequencies ω of light at which zero ellipticity can be measured (we will come back to this question in section 2).

We represent the linear and elliptical polarizations as the real and imaginary portions of a complex quantity. The real value of the rotation angle describes the change of polarization in linearly polarized light. The imaginary value describes the ellipticity of transmitted or reflected light. Once we know the scattering matrix elements r and t on a one-dimensional light propagation problem, then the two characteristic parameters of Faraday/Kerr rotation (Real) and Faraday/Kerr ellipticity (Imaginary) of the magneto-optical transmission/reflection measurements can be written in complex form as the real and imaginary parts of a well-defined complex angle of θ^T and θ^R (see Eqs.(6) and (19)).

In the present paper, we theoretically consider the Faraday rotation of light passing through a RHM/LHM film of thickness L taking into account multiple reflections in the boundaries without absorption. This exactly solvable simple model is chosen to present different aspects of RHM and LHM. It will be shown that the real part of the complex angle of Faraday rotation is an odd function with respect to the refractive index n, while the imaginary part of the angle is an even function of n. We have obtained the rotation angle of backscattered light (Kerr effect) from the RHM/LHM film as well. In the limit of ultra thin LHM film under specific circumstances we will see a large resonant enhancement of the reflected KR angle.

The work is organized as follows. In section 2 we formulate the problem with appropriate analytical expressions for the complex Faraday angle of transmitted light. In section 3 we analyze the Kerr effect and calculate the real and imaginary angles of reflection. In section 4 we study the real and imaginary portions of the complex Faraday rotation angle at different propagation regimes through a finite stack of alternating right and left-handed materials which is analyzed in detail.

2 Right-handed and left-handed dielectric slab

Let us consider a slab confined to the segment $0 \le x \le L$, with a positive impedance $Z = \sqrt{\mu/\epsilon}$ for either RHM or LHM, and characterized by a permittivity $\epsilon = n/Z$ and a permeability $\mu = nZ$. Both n and Z, and therefore ϵ and μ, are frequency dependent complex functions that satisfy certain requirements based on causality. For passive materials, Re(Z) and Im(n) must be greater than zero.

The two semi-infinite media outside the slab are equal and are characterized by the dielectric constant ϵ_1 or by the impedance $Z_1 = \sqrt{\mu/\epsilon_1}$. A linearly polarized electromagnetic plane wave with angular frequency ω enters the slab from the left with normal incidence. We take the direction of propagation as the x axis, and the direction of the electric field $\vec{E}_0$ of the incident wave as the z axis. A weak magnetic field $\vec{B}$, that does not violate the linearity of Maxwell's equations, is applied in the positive x direction and is confined to the slab. This magnetic field causes the direction of linear polarization to rotate while light propagates through the medium. As a consequence, the dielectric tensor develops non-zero off-diagonal elements. Magneto-optic effects are related to the off-diagonal components ϵ_{ij} $(i, j \in \{1, 2\})$, whereas optical properties are related to the diagonal components ϵ_{ii} . The magnitude of the off-diagonal components ϵ_{ij} is two orders of magnitude smaller than that of the diagonal components ϵ_{ii}. The generalized principle of symmetry of kinetic coefficients implies that $\epsilon_{ij}(\vec{B}) = \epsilon_{ij}(-\vec{B})$. The condition that absorption is absent requires that the tensor should be Hermitian $\epsilon_{ij} = \epsilon^{\star}_{ji}$. The latter implies that the real and imaginary parts of ϵ_{ij} must be symmetrical and antisymmetrical, respectively. That is: Re(ϵ_{ij})=Re(ϵ_{ji}) and Im(ϵ_{ij})=-Im(ϵ_{ji}). By combining these conditions with the relation $\epsilon_{ij}(\vec{B}) = \epsilon_{ij}(-\vec{B})$, one can show that the diagonal components of the dielectric tensor are even functions of an applied magnetic field, and the off-diagonal components are odd functions and have first-order magnetic field dependence. The dielectric tensor of

the slab is given by [18]:

$$\epsilon_{ij} = \begin{pmatrix} \epsilon & +ig \\ -ig & \epsilon \end{pmatrix}, \quad (1)$$

where $\vec{g}$ is the gyration vector in the magnetic-field direction. We include the external magnetic field $\vec{B}$ into the gyrotropic vector $\vec{g}$ for our ϵ_{ij}. This way our calculations are valid for the cases of a dielectric in an external magnetic field and for magneto-optical materials.

The components E_z and E_y, H_z and H_y in the film are not constant and depend only on the coordinate x. As well, when a magnetic field is applied in the x direction, the off-diagonal elements ϵ_{ij} cause coupling between the electric field (E_z and E_y) and the magnetic field (H_z and H_y) components. The linearly polarized incident electromagnetic wave can be presented now as the sum of circularly polarized waves with opposite directions of rotation, which propagate through the slab with a different wave vector $k_\pm = \omega n_\pm / c$.

For circularly polarized waves $E_\pm = E_y \pm iE_z$, the Maxwell equations have the form (time variation of optical field is in the form $e^{-i\omega t}$) [18]:

$$\frac{\partial^2 E_\pm}{\partial x^2} + \frac{\omega^2 \epsilon_\pm}{c^2} E_\pm = 0, \quad (2)$$

where $\epsilon_\pm = \epsilon \pm g$.

The reflectance and transmittance amplitudes can be obtained using the continuity of the tangential components of the electric (magnetic) fields at the two interfaces, $x = 0$ and $x = L$. Solving the equations with the appropriate boundary conditions at $x = 0$ and $x = L$ we obtain for the transmitted waves E'_+ and E'_-

$$E'_\pm = E_0 t_\pm,$$

where $t_\pm$ is the transmission amplitude for right and left circularly polarized light and can be presented in the form [18]:

$$t_\pm = T_\pm^{1/2} e^{i\psi_\pm}. \quad (3)$$

The coefficient of transmission $T_\pm$ and the phase $\psi_\pm$ are given by the following expressions, respectively:

$$T_\pm = \left[1 + \frac{1}{4}\left(Z_\pm^{rel} - \frac{1}{Z_\pm^{rel}}\right)^2 \sin^2(\omega L n_\pm / c)\right]^{-1}, \quad (4)$$

$$\tan\psi_\pm = \frac{1}{2}\left(Z_\pm^{rel} + \frac{1}{Z_\pm^{rel}}\right)\tan(\omega L n_\pm / c). \quad (5)$$

Here $Z_\pm^{rel} = \frac{Z_\pm}{Z_1} \equiv \sqrt{\frac{\epsilon_1}{\epsilon \pm g}}$ is the "relative" impedance of a planar dielectric slab of thickness L, characterized by $Z_\pm = \sqrt{\frac{\mu}{\epsilon \pm g}}$, surrounded by two semi-infinite media with positive $Z_1 = \sqrt{\frac{\mu}{\epsilon_1}}$.

As it has been proven, there is a linear relation between the real and imaginary parts of $t_\pm$ and between $\ln t_\pm$ and $\psi_\pm$. These are the known linear Kramers-Kronig relations, that can be rewritten in terms of localization length and density of states [19]. The complex FR angle with the imaginary and real parts is introduced as (see, *e.g.*, [20]):

$$\theta^T = -\frac{i}{2}\ln\frac{t_+}{t_-} = \frac{\psi_+ - \psi_-}{2} - \frac{i}{2}\ln\frac{T_+^{1/2}}{T_-^{1/2}} \equiv \theta_1^T + i\theta_2^T. \quad (6)$$

As we can see from Eq. (6), if $T_+ = T_-$, then $\theta^T \equiv \theta_1^T$ and would only have real component; this signifies that the wave remains linearly polarized with vector $\vec{E}$ rotated an angle θ^T to the initial direction. In the Faraday geometry (a magnetic field is applied parallel to the direction of light propagation) and in the absence of material losses within a thin film, ($R + T = 1$, where R is the reflection coefficient), we have that $T_+ = T_-$ if: (i) the sample is infinite (no boundaries), (ii) for certain thicknesses where total transmission occurs ($T = 1$) or (iii) $n\frac{\partial T^{1/2}}{\partial n} = Z\frac{\partial T^{1/2}}{\partial Z}$. This third condition implies that at certain thicknesses the imaginary portion θ_2^T becomes zero (the solutions following from the transcendental equation, $x_0 = \frac{Z^2+1}{Z^2-1}\tan x_0$). At these points the transmission coefficient T is not one, and its value decreases with increasing x_0, having a saturated value of $4Z^2/(Z^2+1)^2$ when x_0 tends ∞, in contrast to the two previous cases. This saturated value corresponds exactly to one-quarter wavelength.

If $T_+ \neq T_-$, the light is not simply linearly polarized. It has an elliptical polarization, being the ratio of the ellipse semi-axis determined by the relation ($b < a$):

$$\frac{b}{a} = |\tan\theta_2^T| = \frac{\left|T_+^{1/2} - T_-^{1/2}\right|}{\left|T_+^{1/2} + T_-^{1/2}\right|}, \quad (7)$$

where the angle between the large axis of the ellipse and the y axis is:

$$\theta_1^T = \frac{\psi_+ - \psi_-}{2}. \quad (8)$$

For bulk (isotropic) samples or optical devices, where one-way light propagation is important, $\psi_\pm = \omega L n_\pm / c$ (see Eq. 5 when $Z_\pm^{rel} \to 1$). Then, for $Z_\pm^{rel} \approx 1$ the angle θ_1^T reads:

$$\theta_1^T \approx \frac{L\omega\sqrt{\mu}}{2c}\left(\sqrt{\epsilon + g} - \sqrt{\epsilon - g}\right). \quad (9)$$

It can be increased the rotation angle of the linear polarization of θ_1^T on a small length scale in some ways: (i) by taking into account the multiple reflections in a finite layer or resonant structures that can lead to an enhancement of the FR angle (for example Fabry-Perot cavities filled with a magneto-optic material [21]), (ii) tuning the optical properties of ϵ, μ and g by the modification of the structure,

size and shape of the material; varying the composition of alloyed and intermetallic nanostructures, (iii) using metamaterials to tailor the optical properties of the host system [22] (iv) and changing the dielectric permittivity tensor of a medium with time, etc. The time dependence case may concern both the diagonal and non-diagonal permittivity terms of ϵ_{ij} (see Ref. [23]).

In Ref. [22] the permittivity tensor of a magneto-optical metamaterial is tailored by embedded wire meshes. These wires can only tune the diagonal element of the permittivity tensor in terms of topological parameters and material properties. This reduces ϵ to the value of g, creating a near zero epsilon (NZE) metamaterial [24]. For such frequencies the second term of Eq. (9) becomes zero and θ_1^T in the magneto-optical metamaterial can be enhanced by almost an order of magnitude [22]. As well, when Faraday rotation has a time dependent dielectric permittivity tensor, where $g = g_o \cos(\Omega t)$, (being Ω the angular frequency of the gyrotropic vector), it can be shown that the time dependent Faraday rotational angle contains an extra term (proportional to time t and to the frequency ratio $\frac{\omega}{\Omega}$) which increases faster than the stationary term and becomes dominant in short time spans, provided that $\omega t > 1$ [23]).

2.1 Real part of FR in RHM/LHM: Transmission

Let us consider the FR for transmission from a slab. Since the Faraday effect is typically very small the effective indices of refraction and impedance for the two circular polarizations of the first order in g can be presented in the form

$$n_\pm = \sqrt{\epsilon_\pm \mu} \approx n \pm \frac{1}{2}\frac{gn}{|\epsilon|},$$

$$Z_\pm = \sqrt{\mu/\epsilon_\pm} \approx Z \mp \frac{1}{2}\frac{gZ}{|\epsilon|},$$

where n (refractive index of a homogeneous material) and Z (impedance of a homogeneous material) are calculated when gyration vector $\vec{g}$ is zero. Note that by replacing $n \to -n$ we can use the above expressions for LHM.

One can simplify the analysis of θ_1^T and θ_2^T by expanding $\psi_\pm$ around n and Z of the slab in the absence of the magnetic field $\vec{B}$. Then the Taylor series of $T_\pm^{1/2}$ and $\psi_\pm$ in the neighborhood of n and Z becomes:

$$T_\pm^{1/2} = T^{1/2}(n,Z) \pm \frac{1}{2}\frac{gn}{\epsilon}\frac{\partial T^{1/2}}{\partial n} \mp \frac{1}{2}\frac{gZ}{\epsilon}\frac{\partial T^{1/2}}{\partial Z}, \tag{10}$$

$$\psi_\pm = \psi(n,Z) \pm \frac{1}{2}\frac{gn}{|\epsilon|}\frac{\partial \psi}{\partial n} \mp \frac{1}{2}\frac{gZ}{|\epsilon|}\frac{\partial \psi}{\partial Z}. \tag{11}$$

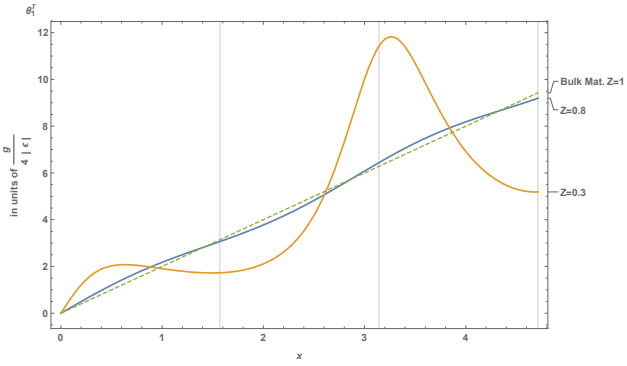

Figure 1: Faraday Rotation angle θ_1^T as a function of $x = \omega nL/c$ for $Z = 0.3$ and $Z = 0.8$ (colour online).

Hence,

$$\theta_1^T = \frac{\psi_+ - \psi_-}{2} = \frac{1}{2}\frac{gn}{|\epsilon|}\frac{\partial \psi}{\partial n} - \frac{1}{2}\frac{gZ}{|\epsilon|}\frac{\partial \psi}{\partial Z} = \frac{1}{2}\frac{g}{|\epsilon|}\left(n\frac{\partial \psi}{\partial n} - Z\frac{\partial \psi}{\partial Z}\right). \tag{12}$$

Evaluating the derivatives $\frac{\partial \psi}{\partial n}$ and $\frac{\partial \psi}{\partial Z}$ at $\vec{B} = 0$ from Eq. 5, substituting these expressions into Eq. 12 and introducing the new parameter $x = \omega nL/c$, we get

$$\theta_1^T = \frac{g}{4|\epsilon|Z}\frac{x(Z^2+1) + (1-Z^2)\sin x \cos x}{1 + \frac{1}{4}\left(Z - \frac{1}{Z}\right)^2 \sin^2 x}. \tag{13}$$

Eq. (13) is a general expression and is valid for any continuous material with arbitrary parameters L, n and Z. As expected, θ_1^T is odd in n and there is a change of the sign of n in LHM. Below we analyze a few of the limits for these parameters.

When L tends to zero ($kL \ll 1$) , the above equation reduces to

$$\theta_1^T \approx \frac{g}{2\epsilon Z}x \equiv \frac{g\omega L}{2c}\frac{\epsilon}{|\epsilon|}, \tag{14}$$

which coincides with the thin-film result of Ref. [25] for RHM ($\epsilon > 0$).

If $Z = 1$, *i.e.* when light propagates in an homogenous medium, we get

$$\theta_1^T = \frac{g}{2|\epsilon|}x \equiv \frac{g\omega L}{2c|\epsilon|}\sqrt{\mu\epsilon}, \tag{15}$$

which coincides with the result of Refs. [18, 25] in the thick film limit where $kL \gg 1$, for $\mu = 1$ in RHM and for the range of all optical frequencies. At the points $x_0 = \frac{Z^2+1}{Z^2-1}\tan x_0$, where the ellipticity is zero ($\theta_2^T = 0$), as was mentioned previously, we get for the real part of FR:

$$\theta_1^T = \frac{gZ}{|\epsilon|(Z^2+1)}x_0 \tag{16}$$

In Figure 1 we show the FR angle of transmission vs $x = \omega nL/c$ for RHM, using Eq. (13) for three different values of surface impedance: $Z = 0.3$, $Z = 0.8$, and bulk material with no reflections where $Z = 1$ (dashed line). The angle steadily increases and oscillates around the line $\theta_1^T = 2x$ (in units $\frac{g}{4|\epsilon|}$ with certain periodicity of π or on the scale $L \sim k^{-1}$). The oscillations in θ_1^T are due to interference effects in the plane-parallel slab and the amplitude of the oscillating part depends on x. At $x_l = \pi(l + 1/2)$ $(l = 1, 2 \ldots)$ we have for FR angle $\theta_1^T = \frac{gZ}{|\epsilon|}\frac{x_l}{Z^2+1}$, and for $x_l = \pi l$ we have $\theta_1^T = \frac{g}{4|\epsilon|}\frac{Z^2+1}{Z}x_l$. We were not able to find an analytically closed-form solution for the maximum of θ_1^T, and Eq. (13) could not calculate the maximum increase of FR angle. However, for the estimated increase we used points $x_l = \pi l$, because the maximum value of θ_1^T for each period of oscillation is located very close to that points (see Fig. 1 where the vertical grid line appears). Then the ratio of θ_1^T at $x_l = \pi l$ to the θ_1^T in homogeneous media, Eq. (15), reads $(Z^2 + 1)/2Z \geq 1$. For materials with relative impedance ~ 0.3, such as semiconductors with zero extinction coefficients in the near or mid infrared range (like tellurium or aluminum gallium arsenide), the ratio can be almost 2. That is, an impedance $z < 1$ causes multiple reflections that increase the overall time the light spends within the system, showing an increase in Faraday rotation [20]. A similar increase of Faraday rotation was also found in [22, 26]. However, for a composite system (dielectric with metamaterials or super lattice systems) the effective ϵ can be reduced up to 10^{-2} and the ratio can thus be increased by an order of magnitude or greater.

2.2 Imaginary part of FR in RHM/LHM: Transmission

Expanding $T_{\pm}^{1/2}$ around n and Z of the slab in the absence of the magnetic field $\vec{B}$ (see Eq. (10) by using the Taylor series for $\ln(1 + x)$ centered at 0, we can similarly derive the expression for $\theta_2^T = \frac{1}{2}\ln\frac{T_+^{1/2}}{T_-^{1/2}}$ for the imaginary portion of Faraday rotation as:

$$\theta_2^T = \frac{g}{8|\epsilon|Z^2}\frac{(1-Z^2)\sin x\left[(Z^2+1)\sin x + x(1-Z^2)\cos x\right]}{1+\frac{1}{4}\left(Z-\frac{1}{Z}\right)^2\sin^2 x}. \quad (17)$$

This is again a general expression valid for the arbitrary parameters L, n and Z. As expected, θ_2^T is even in n, and $\theta_2^T \to 0$ when L tends to zero. As it was previously mentioned, θ_2^T becomes 0 at $Z = 1$ (no boundaries), at $x = \pi l$ (complete transmission) and at $x_0 = \frac{Z^2+1}{Z^2-1}\tan x_0$. In the two former cases the coefficient of transmission T becomes 1 when an external magnetic field $\vec{B}$ is zero. The third case is very different: The transmission coefficient is not 1 and instead T approaches $4Z^2/(Z^2 + 1)^2$ as x_0 tends ∞. This saturated value corresponds exactly to one-quarter wavelength.

Note that in the limit of a small magnetic field $\vec{B}$ the expression for $\frac{b}{a}$, Eq. (7), coincides with θ_2^T defiend by Eq. (17).

Figure 2 shows the imaginary angle of the FR in Eq. (17) for a RHM $(n > 0)$ versus x, for materials with $Z = 0.3$ (solid) and $Z = 0.8$ (dashed). θ_2^T in the interval $[0, \pi]$ increases with x, reaches a peak value and then drops to a minimum. This pattern repeats as x increases. Let us finally remark that from Figure 1 and Figure 2 it follows that the maximums of the real portions of the Faraday effect do not coincide with the simultaneously zero imaginary portions.

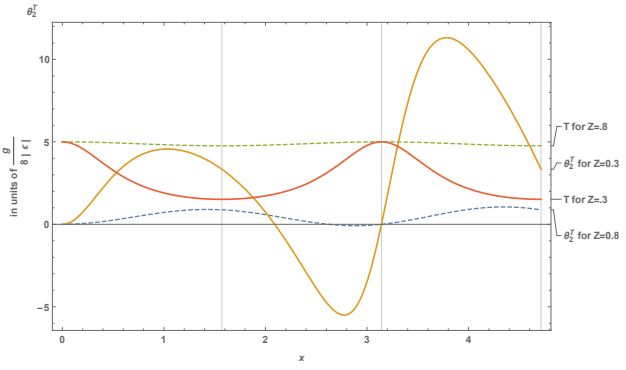

Figure 2: Faraday Rotation angle θ_2^T as a function of $x = \omega nL/c$ for Z=0.3 and Z=0.8. Transmission is multiplied by 5 to highlight the relationship between the Faraday ellipticity angle and corresponding transmission value, where $T = 1$ is the norm (colour online).

3 Real and Imaginary parts of KR in RHM/LHM: Reflection

When linearly polarized light is reflected from the surface of a magnetized material, the direction of polarization changes and the light can be elliptically polarized. This is the Kerr effect, very similar to the Faraday effect with the exception that the Kerr effect refers to the reflection of light and the Faraday effect refers to its transmission.

Before analizing the complex Kerr effect in more detail, let us note that if we ignore the losses there are some useful results which relate the θ^T and θ^R which follow from the general expressions of the scattering matrix elements in terms of the transmission and reflection probabilities

and the scattering phases ψ and $\psi \pm \psi_a$. Here ψ is the total phase accumulated in a transmission event and $\psi \pm \psi_a$ are the phases accumulated by a particle which is incident from either face of the material when it is reflected. The scattering-matrix elements can be written in the form:

$$S = \begin{pmatrix} r & t \\ t & r' \end{pmatrix} = \begin{pmatrix} -i\sqrt{R}e^{i(\psi+\psi_a)} & \sqrt{T}e^{i(\psi)} \\ \sqrt{T}e^{i(\psi)} & -i\sqrt{R}e^{i(\psi-\psi_a)} \end{pmatrix}$$

.

For a spatially symmetric barrier the phase asymmetry ψ_a vanishes and $r = r'$. It is clear that for any symmetric structure with no material losses, including the slab we are discussing,

$$\theta_1^R = \theta_1^T.$$

Whereas $t_\pm$ describes the transmission amplitude of the wave, we now describe $r_\pm$ as the reflection amplitude. It can be shown for the slab that the reflection amplitude is given by [18]:

$$r_\pm = -i\frac{t_\pm}{2}(Z_\pm - \frac{1}{Z_\pm})\sin(n_\pm \omega L/c), \tag{18}$$

where $t_\pm$ was defined in Eq. (3). Using an expression similar to that of FR to describe the Kerr effect complex rotation angle we find that,

$$\theta^R = -i \ln \frac{r_+}{r_-} = \theta_1^R + i\theta_2^R, \tag{19}$$

and,

$$\theta_2^R = \theta_2^T - \frac{g}{2\epsilon}\left(\frac{(nkL)\cos(nkL)}{\sin(nkL)} + \frac{Z^2+1}{1-Z^2}\right), \tag{20}$$

where θ_2^T is defined by Eq. (17).

When L tends to zero (the thin film approximation), the above expression reduces to

$$\theta_2^R \approx \frac{\epsilon}{|\epsilon|}\frac{g}{\epsilon - \mu},$$

where epsilon has a sign change from RHM to LHM.

As it can be seen in the above expression, θ_2^T is proportional to the extremely small parameter g and in RHM, where $\mu \ll \epsilon$, it is too difficult to measure θ^R. However, the situation is very different for LHM, where μ and ϵ can be of the same order of magnitude for some frequency ranges (as for NZE metamaterials). For these frequencies it can be verified experimentally that a narrow resonantly enhanced reflection angle can be found for the Kerr effect.

Figure 3 shows the imaginary angle of the KR, Eq. (20), for two different RHM of different surface impedance Z versus x . θ_2^R at $x_l = \pi l$ shows a discontinuity. We also note that zeroes for both θ_2^T and θ_2^R coincide and are the solutions to the transcendental equation $x_0 = \frac{Z^2+1}{Z^2-1}\tan x_0$. At these points there is linearly polarized light for both the reflected and transmitted light.

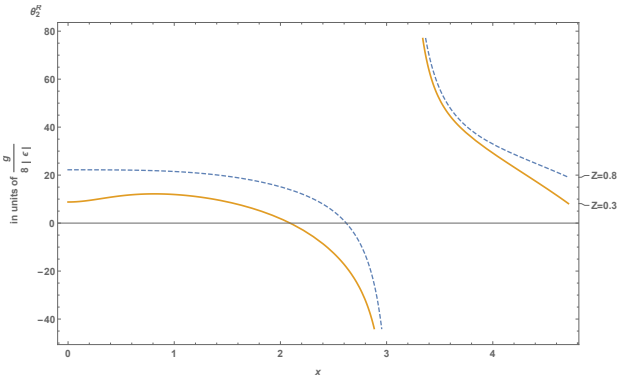

Figure 3: Kerr Rotation angle θ_2^R as a function of $x = \omega nL/c$ for $Z = 0.3$ and $Z = 0.8$ (colour online).

4 Alternating right and left-handed materials: layered structures

In this section we shall analyze in detail the real and imaginary portions of the complex Faraday rotation angle at the different propagation regimes through a finite stack of alternating right and left-handed materials ($n_1 > 0$ and $n_2 < 0$, respectively). In such systems, the total Faraday rotation is defined as the rotation of the resultant superposition of the transmitted electric fields $E_\pm$ that experience multiple reflections, as discussed previously for a single film. The mentioned multiple reflections along different trajectories, corresponding to different traversal times, can lead to evanescent modes of so-called "superluminal velocities" on microwave transmission through an undersized waveguide [27, 28] or periodic dielectric heterostrucures [29, 30]. It is widely believed that the evanescent modes take almost zero time to cross the forbidden region and for an opaque barrier, where there is a strong exponential decay of the wave function, the tunneling time becomes independent of the barrier's length (known as the Hartman effect [31]). However, a very fast tunneling, or a zero tunneling time holds a serious consequence: the tunneling velocity or the average velocity may become higher than the velocity of light c. Indeed, following the standard definition of the phase time, $t = \hbar\frac{d\varphi}{dE}$ (where time elapses between the peak of the wavepacket entering the barrier and leaving it), it is easy to be convinced that for evanescent modes one will get a very fast tunneling time.

Without pretending to give an exhaustive review on the theory of the traversal time problem of electromagnetic waves, we just mention that two characteristic times have arisen in many approaches (see for example, Refs. [32, 33] and references therein). These times are related as a consequence of the analytical properties of the complex quantity

whose real and imaginary components are the two characteristic times. However, as we know, any experiment must measure a real quantity, and so the outcome of any measurement of the interaction time must be a real quantity, possibly involving the two characteristic times. It depends on the experimente which of the two components of this interaction time is the most relevant.

We can see in the experiment performed in Ref. [34] an example of a two components interaction time. There it was experimentally investigated the tunneling times associated with frustrated total internal reflection of light. It was shown that the two characteristic times correspond, respectively, to the spatial and angular shifts of the beam.

As a second example, we can mention the magnetic clock approach [20] (Faraday rotation), where the time that characterizes the interaction of a classical electromagnetic wave with a barrier must always be described by two-components of a complex time: $\tau = \tau_1 - i\tau_2$.

The real portion of complex Faraday angle θ is proportional to the traversal time τ_1 of light through the magnetic materials or dielectric structures in an external weak magnetic field [20]. At the same time the imaginary component of complex θ is proportional to the degree of ellipticity, τ_2. Remarkably, the two times τ_1 and τ_2 are related via Kramers-Kronig integral dispersion relation [35] that prevents a violation of the principle of causality. Indeed, the validity of the Kramers-Kronig relations for the complex interaction time has a rather deep significance because it may be demonstrated that these conditions are a direct result of the causal nature of physical systems by which the response to a stimulus never precedes the stimulus [35]. Based on this remark, note that the experiments with, *e.g.*, undersized waveguides [27, 28] or periodic dielectric heterostrucures [29, 30], where the so called "superluminal" have been observed for the barrier tunneling time need to be interpreted very carefully.

To shed some light on the obstacles which have persisted in the tunneling time problem, we analyze the real and imaginary portions of the complex Faraday rotation angle in the forbidden bands of a finite stack of alternating right and left-handed materials. This type of alternating structure, assuming that the optical paths of two slabs are equal to each other ($n_1 L_1 = |n_2| L_2$), exhibits a broad forbidden bands spectrum (see Figure 4a below). This serves as a good candidate and a basis for a qualitative understanding of the peculiarities of complex Faraday rotation, as well as the two-components of the interaction time in a barrier.

For our numerical simulations we have chosen a finite stack of alternating right (refractive index $n_1 = 1.58$ and length $L_1 = 52.92$ nm) and left-handed (refractive index $n_2 = -2.12$ and length $L_2 = 39.38$ nm) materials. The wave-numbers in the layers of both types are $k_i = \omega n_i / c$, where ω is the frequency and c the vacuum speed of light. Due to the high contrast between the two dielectrics n_1 and $|n_2|$, 10 primitive cells are already enough to formulate allowed and forbidden band structures. In Figure 4a we present the transmission coefficient T as a function of the frequency ω for single, five, ten and fifty primitive cells.

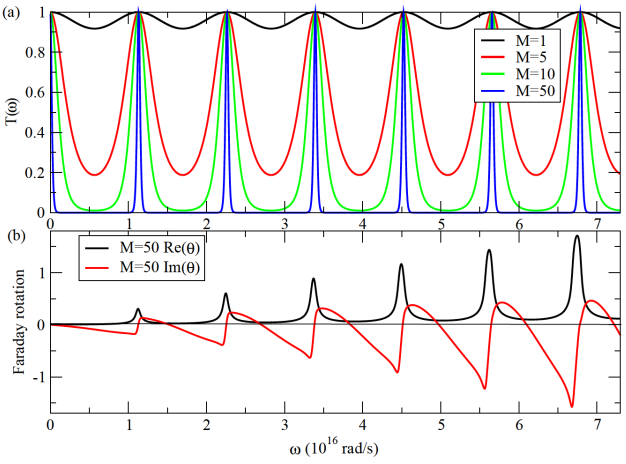

Figure 4: (a)The transmission coefficient and (b) real and imaginary parts of the Faraday Rotation angle θ as a function of ω for an alternating structure described in the text. The parameters are: number of primitive cells $M = 50$, $n_1 = 1.58$, $n_2 = -2.12$, $L_1 = 52.92$ nm, $L_2 = 39.38$ nm and $n_1 L_1 = |n_2| L_2$ (colour online).

The transmission coefficient was calculated by using the characteristic determinant method [36, 37], that allows one to express the transmission coefficient of a wave propagating in a one-dimensional structure through the determinant $T = |D|^{-2}$. The latter depends on the amplitudes of reflection of a single scatterer only. This characteristic determinant approach is compatible with the transfer matrix method and has been widely used to calculate the average density of states over a sample, the energy spectrum of elementary excitations, or the characteristic barrier tunneling time, among others (Ref. [38]).

Having a close look into forbidden and allowed band regions in Figure 4a, one observes that practically the entire transmission spectrum, starting from $M = 10$, is formed by forbidden gaps. Further increase of cells will be narrowing the allowed bands, and in the limit of an ideal infinite crystal one gets a set of periodically distributed Lorentzian resonances. The centers of the $m - th$ allowed band, ω_c can be easily determined via the dispersion relation obtained from the Bloch-Floquet theorem for an ideal

infinite crystal (see, for example, Ref. [15])

$$\omega_c = \frac{c\pi m}{n_1 L_1} \equiv m1.13 \times 10^{16}\text{rad/s}$$

In Figure 4b we present the real and imaginary portions of Faraday complex angle θ for $M = 50$ primitive cells. The maximums of Re(θ) are centered in the allowed bands and coincide with $\omega_c \equiv m1.13\times10^{16}$rad/s. At these resonance peaks $T_- = T_+$ and we deal with the pure Faraday rotation of linearly polarized wave, *i.e.* with no wave ellipticity. Within any forbidden bands, Re(θ) is an almost flat function with a very small value. This is what we expect according to the above discussion on "superluminal velocities" and taking into account the existing deep connection between the Re(θ) and the tunneling time τ_1. However, the situation is completely different for Im(θ) (proportional to the degree of ellipticity) or for τ_2. First, the latter is zero at any allowed band at ω_c where the condition $T_- = T_+$ is satisfied, and jumps from zero to some positive value at the end of the allowed band. Second, in the forbidden gap Im(θ) starts to decrease monotonically with increasing frequency ω changing the sign from positive to negative, and sharply becomes zero in the next allowed band. In forbidden gaps, at the frequencies where Im(θ) becomes zero, T_- is exactly equal to T_+. At these frequencies the electromagnetic waves remain linearly polarized. At the rest of frequencies in the forbidden gap the wave is elliptically polarized and its axis is rotated either in the right or left direction. The dependence of Im(θ) on ω is similar to a sawtooth function with increasing amplitude. By comparing with the stable behaviour of Re(θ) in the forbidden gap, where the latter's value is almost zero, one notes that the Im(θ) changes drastically in both value and sign. The fast rotation of the ellipse semi-axis from a positive to a negative sign in the forbidden gap is connected to the anomalously small value of Re(θ) in the same frequencies range. As a consequence, in the time domain the contribution of τ_2 for evanescent modes is dominant compared to τ_1 in the whole range of a forbidden gap.

5 Conclusion

We have studied in this work the Faraday and Kerr rotations of light with angular frequency ω passing through a RHM/LHM film with thickness L, taking into account the multiple reflections from the boundaries. The descriptions of the real portions as the linear angle of rotation and imaginary portions as the ellipticity of the rotation allow us to separate the two distinct phenomena and visualize their maximums and effects within different kinds of mediums. We found that the rotation and ellipticity of the transmitted or reflected light of the Faraday and Kerr effects are odd and even functions with respect to the refractive index n. These odd and even functions are not just the properties of a thin film, but apply just as well to the case of any system of arbitrary length.

For a spatially symmetric film with no material losses the real portion of Faraday and Kerr rotations are equal for RHM and LHM. However, the imaginary portion of Kerr rotation for LHM has a peculiar behaviour when the symmetric film's length tends to zero. In the limit of an ultra thin LHM film, where ϵ and μ can be of the same order of magnitude for some frequency ranges, it was experimentally detected a large resonant enhancement of the reflected KR angle. It has been shown that the maximums of the real portions of the Faraday effect do not coincide with the simultaneously zero imaginary portions, in contrast to the case of bulk materials.

To shed some light on the obstacles which have persisted in the tunneling time problem, we have analyzed the real and imaginary portions of the complex Faraday rotation angle in the forbidden bands of a finite stack of alternating right and left-handed materials. It has been shown that in spite of the fact that Re(θ) in the forbidden gap is almost zero, the Im(θ) changes drastically in both value and sign.

References

[1] Padilla, W. J., D. N. Basov, and D. R. Smith. Negative refractive index metamaterials. *Materials Today*, Vol. 9, No. 7-8, 2006, pp. 28–35.

[2] Veselago, V. G. The electrodynamics of substances with simultaneously negative values of ϵ and μ. *Soviet Physics - Uspekhi*, Vol. 10, No. 4, 1968, pp. 509–514.

[3] Smith, D. R., W. J. Padilla, D. C. Vier, S. C. Nemat-Nasser, and S. Schultz. Composite medium with simultaneously negative permeability and permittivity. Physical Review Letters, Vol. 84, No. 18, 2000, pp. 4184-4187.

[4] Garcia Pomar, J. L., Negative and anomalous refraction in metamaterials and photonic crystals, PhD thesis, Madrid, Spain, 2009.

[5] Smith, D. R., J. B. Pendry, and M. C. K. Wiltshire. Metamaterials and negative refractive index. *Science*, Vol. 305, No. 5685, 2004, pp. 788–792.

[6] Pendry, J. B. Negative refraction makes a perfect lens. *Physical Review Letters*, Vol. 85, No. 18, 2000, pp. 3966–3969.

[7] Yang, S., P. Liu, M. Yang, Q. Wang, J. Song, and L. Dong. From Flexible and Stretchable Meta-Atom to Metamaterial: A Wearable Microwave Meta-Skin with Tunable Frequency Selective and Cloaking Effects. *Scientific Reports*, Vol. 6, No. 1, 2016, id. 21921.

[8] Schurig, D., J. J. Mock, B. J. Justice, S. A. Cummer, J. B. Pendry, A. F. Starr, and D. R. Smith. Metamaterial electromagnetic cloak at

microwave frequencies. *Science*, Vol. 314, No. 5801, 2006, pp. 977–980.

[9] Leonhardt, U. Optical conformal mapping. *Science*, Vol. 312, No. 5781, 2006, pp. 1777–1780.

[10] Yang, Y., J. Xu, H. Chen, and S. Zhu. Quantum interference enhancement with left-handed materials. *Physical Review Letters*, Vol. 100, No. 4, 2008, id. 043601.

[11] Papasimakis, N., and N. I. Zheludev. Metamaterial-induced transparency: Sharp Fano resonances and slow light. *Optics and Photonics News*, Vol. 20, No. 10, 2009, pp. 22–27.

[12] Zhang, L., S. Liu, L. Li, and T. J. Cui. Spin-Controlled Multiple Pencil Beams and Vortex Beams with Different Polarizations Generated by Pancharatnam-Berry Coding Metasurfaces. *Appl. Mater. Interfaces*, Vol. 9, No. 41, 2017, pp. 36447–36455.

[13] Ahamed, E., M. R. I. Faruque, M. J. Alam, M. F. B. Mansor, and M. T. Islam. Digital metamaterial filter for encoding information. *Scientific Reports*, Vol. 10, No. 1, 2020, id. 3289, DOI: 10.1038/s41598-020-60170-8.

[14] Asatryan, A. A., L. C. Botten, M. A. Byrne, V. D. Freilikher, S. A. Gredeskul, I. V. Shadrivov, et al. Suppression of Anderson localization in disordered metamaterials. *Physical Review Letters*, Vol. 99, No. 19, 2007, id. 193902.

[15] del Barco, O., and M. Ortuño. Localization length of nearly periodic layered metamaterials. *Physical Review A*, Vol. 86, No. 2, 2012, id. 023846.

[16] del Barco, O., V. Gasparian, and Z. Gevorkian. Localization-length calculations in alternating metamaterial-birefringent disordered layered stacks. *Physical Review A*, Vol. 91, No. 6, 2015, id. 063822.

[17] Torres-Herrera, E. J., F. M. Izrailev, and N. M. Makarov. Non-conventional Anderson localization in a matched quarter stack with metamaterials. *New Journal of Physics*, Vol. 15, No. 5, 2013, id. 055014.

[18] Landau, L. D., and E. M. Lifshitz. Electrodynamics of Continuous Media, Elsevier, United Kingdom, 1984.

[19] Thouless, D. Electrons in disordered systems and the theory of localization. *Physics Reports*, Vol. 13, No. 3, 1974, pp. 93-142.

[20] Gasparian, V., M. Ortuño, J. Ruiz, and E. Cuevas. Faraday rotation and complex-valued traversal time for classical light waves. *Physical Review Letters*, Vol. 75, No. 12, 1995, pp. 2312–2315.

[21] Inoue, M., K. Nishimura, and T. Fujii. Localization and hopping of magnetoelastic waves in highly magnetostrictive strings with random chain structures (abstract). *Journal of Applied Physics*, Vol. 81, No. 8, 1997, id. 5692.

[22] Sadatgol, M., M. Rahman, E. Forati, M. Levy, and D. O. Guney. Enhanced Faraday rotation in hybrid magneto-optical metamaterial structure of bismuth-substituted-iron-garnet with embedded-gold-wires. *Journal of Applied Physics*, Vol. 119, No. 10, 2016, id. 103105.

[23] Gevorkian, Z., V. Gasparian, and J. Lofy. Time dependent Faraday rotation. *Laser Physics*, Vol. 28, No. 1, 2018, id. 016001.

[24] Caligiuri, V., R. Dhama, K. V. Sreekanth, G. Strangi, and A. De Luca. Dielectric singularity in hyperbolic metamaterials: The inversion point of coexisting anisotropies. *Scientific Reports*, Vol. 6, No. 1, 2016, id. 20002.

[25] Gevorkian, Z., and V. Gasparian. Plasmon-enhanced Faraday rotation in thin films. *Physical Review A.*, Vol. 89, No. 2, 2014, id. 023830.

[26] Sharipova, M., A. I. Musorin, T. D. Dolgova and A. Fedyanin. Ultrafast dynamics of Faraday rotation in thin films. Proceedings SPIE Optics+Optoelectronics, Prague, Czech Republic, Vol. 9502, 2015. Available from: DOI: 10.1117/12.2180635

[27] Enders, A., and G. Nimtz. On superluminal barrier traversal. *Journal de Physique I*, Vol. 2, 1992, pp. 1693–1698.

[28] Enders, A., and G. Nimtz. Evanescent-mode propagation and quantum tunneling. *Physical Review E*, Vol. 48, 1993, pp. 632–634.

[29] Steinberg, A. M., P. G. Kwiat, and R. Y. Chiao. Measurement of the single-photon tunneling time. *Physical Review Letters*, Vol. 71, No. 5, 1993, pp. 708–711.

[30] Spielman, Ch., R. Szipöcs, A. Stingl, and F. Krausz. Surface roughness scaling of plasma polymer films. *Physical Review Letters*, Vol. 73, 1994, pp. 708-711.

[31] Hartman, E. Tunneling of a Wave Packet. *Journal of Applied Physics*, Vol. 33, No. 12, 1962, pp. 3427–3433.

[32] Gasparian, V., M. Ortuño, G. Schön, and U. Simon. *Handbook of Nanostructured Materials and Nanotechnology*, Vol. 2, Nalwa, H. S., Ed. Academic Press, New York, 2000, pp. 513–569.

[33] Muga, J. G., and C. R. Leavens. Arrival time in quantum mechanics. *Physics Reports*, Vol. 338, No. 4, 2000, pp. 353–438.

[34] Balcou, Ph., and L. Dutriaux. Dual Optical Tunneling Times in Frustrated Total Internal Reflection. *Physical Review Letters*, Vol. 78, No. 5, 1997, pp. 851–854.

[35] Gasparian, V., J. Ruiz, G. Schön, and M. Ortuño. Kramers-Kronig relations and the barrier interaction time problem. *European Physical Journal B*, Vol. 9, No. 2, 1999, pp. 283–287.

[36] Aronov, A. G., V. M. Gasparian, and U. Gummich. Transmission of waves through one-dimensional random layered systems. *Journal of Physics Condensed Matter*, Vol. 3, No. 17, 1991, pp. 3023–3039.

[37] Gasparian, V. Sov. Phys. Solid State 31 (1989) 266. *Fiz. Tverd. Tela*, Vol. 31, 1989, p. 162.

[38] Carpena, P., V. Gasparian, and M. Ortuño. Finite periodic and quasiperiodic systems in an electric field. *Zeitschrift für Physik B, Condensed Matter*, Vol. 102, No. 3, 1997, pp. 425–431.